Chemosphere 363 (2024) 142906

Contents lists available at ScienceDirect

Chemosphere

journal homepage: www.elsevier.com/locate/chemosphere

Assessment of atmospheric pollution by potentially toxic elements in the urban areas of the Riotinto mining district

Annika Parviainen [a,*], Carolina Rosca [b], Deyanira Rondon [b], Manuel Casares Porcel [c], Francisco José Martín-Peinado [a]

[a] Universidad de Granada, Departamento de Edafología y Química Agrícola, Avda. Fuente Nueva s/n, E-18071, Granada, Spain
[b] Instituto Andaluz de Ciencias de la Tierra (CSIC), Avda. de las Palmeras 4, E-18100, Armilla, Granada, Spain
[c] Universidad de Granada, Departamento de Botánica, Campus Universitario de Cartuja, E-18071, Granada, Spain

HIGHLIGHTS

- Metal(loid)s were studied in lichen bioindicators in urban areas of mining towns.
- High bioaccumulation of sulfide-associated elements was observed in *Xanthoria* parietina.
- Ratios of Cu, Zn, As and Pb were distinct from traffic-related pollution sources.
- Potentially toxic elements were significantly higher in mining towns than control towns.

GRAPHICAL ABSTRACT

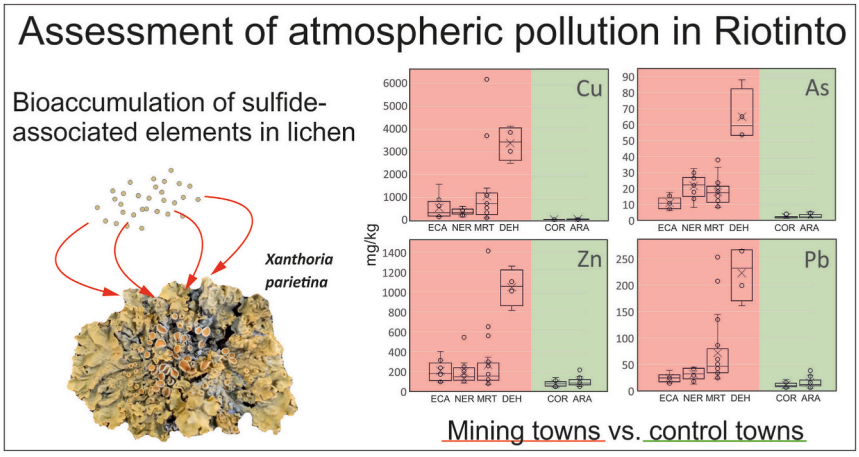

ARTICLE INFO

Handling editor: R Ebinghaus

Keywords:
Xanthoria parietina
Bioindicator
Arsenic
Lead
Atmospheric pollution

ABSTRACT

Ore mineralizations in bedrock and their exploitation may have a negative impact on air quality of surrounding urban areas and, subsequently, on human health. This study uses lichens as bioindicators of atmospheric pollution to evaluate the spatial distribution of potentially toxic elements (PTEs) in the towns close to the massive sulfide deposits of the Iberian Pyrite Belt (IPB) in SW Spain. Altogether 89 native lichen samples of *Xanthoria parietina* were collected from the mining towns, control towns out of the reach of the mining activity, as well as from distal sampling sites. The samples were analyzed for 29 elements after acid digestion. The concentrations for Co, Ni, Cu, Zn, As, Rb, Mo, Cd, Sn, Sb, Cs, Ba, W, Tl, Pb, S, and Fe are significantly higher in the mining towns in comparison to the control towns. The ore mineral-associated PTEs, including Cu, Zn, As, Ba, and Pb, exhibit extreme concentrations in the urban areas close to the mining activity, and particularly in the small settlement of La Dehesa next to the mineral processing plant and the tailings pond. The distal samples confirm

* Corresponding author.
E-mail addresses: aparviainen@ugr.es (A. Parviainen), carolina.rosca@csic.es (C. Rosca), deyanira.rondon@csic.es (D. Rondon), mcasares@ugr.es (M. Casares Porcel), jmartin@ugr.es (F.J. Martín-Peinado).

https://doi.org/10.1016/j.chemosphere.2024.142906
Received 5 June 2024; Received in revised form 17 July 2024; Accepted 18 July 2024
Available online 21 July 2024

the decrease in the concentrations of all PTEs, and these samples present similar values as in the control areas. The results, point at increased bioaccumulation of PTEs in the lichen thalli of the adjacent urban areas, suggesting that the air quality of the adjacent urban areas is locally impacted by the massive polymetallic sulfide deposits which is enhanced by the mining activity. Therefore, monitoring the urban air quality is recommended.

1. Introduction

The demand for mineral and metal raw materials is expected to increase in the future due to the decarbonization of the energy supplies and the consequent transition to so-called green energies including solar panels, wind turbines, and electric cars among other applications (OECD, 2019). This projection implies the growth of the extractive industry, which may subsequently lead to increasing environmental hazards. Atmospheric pollution is one of the principal dispersion routes of potentially toxic elements (PTEs) from mining activities to the surrounding soil, water, and air, and it is a major concern for public health. In addition, PTE mobilization through mining spills and generation of acid mine drainage have received intense research interest in the past decades (Nieto et al., 2013). Therefore, monitoring and understanding the different routes of pollution and human exposure are of uttermost interest.

Lichens are robust biomonitors of atmospheric pollution and they have been widely used to study urban areas and also the impacts of mining and related industries (Jiménez-Moreno et al., 2016; Kováčik et al., 2023; Parviainen et al., 2019, 2020; Widory et al., 2018). Depending on the stability of the substrate and the species, the longevity of lichens can vary from decades to centuries (Branquinho, 2001). In the case of corticolous lichens, the substrate can change due to the growth in thickness of the trunks and the variation in lighting conditions due to the growth of the crown. Long-term species survival may vary depending on the tree species and lichen tolerance. Although there are few studies on the survival of corticolous species, in most cases it can be estimated that their life expectancy is several decades (Rasmussen et al., 2018). For the species considered in this study, the growth rate can be estimated at approximately 1–3 mm per year (Fortuna and Tretiach, 2018). Due to the radial growth of foliose lichens, the older, inner parts of the lobe accumulate the highest elemental concentrations, whereas the newer peripheral parts reflect the recent bioaccumulation. In the absence of roots, cuticula, stromata and excretion mechanisms, lichens passively catch the nutrients form ambient air, and therefore the PTE concentrations proportionally reflect the concentrations in the atmosphere. PTEs are deposited in lichens through rain, fog or dew and through dry deposition of airborne particulate matter (PM) (Knops et al., 1991). The understanding of the intimate nature of the absorption and accumulation process is still scarce, however there are numerous evidences that the elemental concentrations in lichens correlate with those of the environment (Conti and Cecchetti, 2001). Their ability to remain in one place for extended periods allows the PTE composition of the environment to be evaluated over time. Native or transplanted lichens can be used for biomonitoring (Cecconi et al., 2019; Francová et al., 2017; Saib et al., 2023). Some toxitolerant species like *Xanthoria parietina* (L.) Th. Fr. are especially very common in urban areas, making them affordable and easy sample materials to collect. They also present the advantage of allowing the collection of a dense sample grid as opposed to expensive PM monitoring systems. Hence, they are excellent bioindicators of atmospheric pollution, and they show potential for assessing the spatial distribution of PTEs surrounding mining areas.

Even though a direct relation between chemical composition of lichens and airborne PM can be expected, this topic is underexplored. There are only few studies that compare the lichen chemistry with samples from PM collectors. Atmospheric PM in an uncontaminated area in Italy has been proven to present good correlation with transplanted *Pseudoevernia furfuracea* corroborating the efficacy of lichens as robust bioindicators of atmospheric pollution (Bari et al., 2000). Concentrations of Pb, Zn, and Cd in PM collectors have also been reported to have a good positive correlation with transplanted *Flavocetraria nivalis* in a mining area in Greenland (Søndergaard et al., 2013).

The Riotinto region in the Province of Huelva (SW Spain) is a world-renowned mining area with mining history dating back to as early as pre-Roman times and the activity peaked in the 20th century (Nocete et al., 2014). Mining ceased temporally from 2000 to 2015, but currently the open pit at Cerro Colorado is being exploited for Cu and Ag with an estimated life-of-mine of over 15 years (Atalaya Minining, 2023). The areas affected by mining including open pits and various kinds of mining wastes cover roughly 25 km^2. The aim of this study was to assess the spatial distribution of PTEs in the atmosphere of the urban areas located in the proximities of the Riotinto mining district and compare the metal (loid) levels with control areas from the northern part of the Province of Huelva, far away from the mining activity. We also aimed to compare our results with previous PM data from the study area and lichen studies from other urban areas with different pollution sources as an attempt to discriminate mining activity and traffic related sources. To our knowledge this is the first attempt to compare PM chemistry with native *Xanthoria parietina*. This work enables a better understanding of the potential risk areas for chronic human exposure to atmospheric pollution with a more comprehensive and exhaustive evaluation of the mining and control areas than before.

2. Materials and methods

2.1. Study area and sampling

This study focuses on the mining area of Riotinto in the central part of the Province of Huelva in SW Spain. The northern part of the province was chosen as a control area (Fig. 1). These areas are very different in terms of the geology and lithology. The study area in Riotinto lies within the geological complex of South Portuguese Zone. This zone hosts the world known ore deposits of the Iberian Pyrite Belt (IPB) with original ore reserves of >1500 Mt (Sáez et al., 1999). The massive sulfide and polymetallic ore deposits of IPB are hosted in volcano-sedimentary rocks. The Riotinto area has an active mining history since Roman times until year 2000. The mining activity revived in 2015 and has future prospects for over 15 years (Atalaya Minining, 2023). The open pit at Cerro Colorado is currently being exploited and there are several other closed workings including Corta Atalaya, Peña del Hierro, and Zarandas (Fig. 1). The Northern part of the province is characterized by the Ossa Morena Zone, where the control areas investigated in this study are located in the Metamorphic Belt of Aracena. This area lacks large scale mining and merely some small historical mining activity has been recorded (Ruiz de Almodóvar Sel and Pérez López, 2008).

Native lichen samples of the species *Xanthoria parietina* were collected in January 2022 from the urban areas, with a special focus on the public parks and green areas. Samples were collected from the study area in the close vicinity of the mining activities (N = 47) covering the towns of El Campillo (2018 inhabitants in 2022 according to Andalusian Institute of Statistics and Cartography, 2022), Minas de Riotinto (3738), La Dehesa (266; small settlement of Minas de Riotinto), and Nerva (5100) and from control areas out of the area of exposure of the mines (N = 33) in Cortegana (4636) and Aracena (8240). Additionally, distal samples (N = 9) were collected in different wind directions from the mining area to evaluate a potential attenuation effect of the metal(loid) concentrations in the atmosphere. Samples were collected approximately every 5 km until reaching 20–30 km distance from Riotinto. The

coordinates and description of the sampling sites can be found in the Supplementary Table S1. The lichen samples were retrieved using a plastic knife, that was cleaned with alcohol in between samples, and saved in metal-free plastic tubes. The outermost 5 mm of the peripheral part of the lichens was collected representing approximately the growth of the latest 4 years due to the rate of radial growth (Fortuna and Tretiach, 2018). In cases where small lichens (<10 mm in diameter) were found, the whole thalli were collected. According to Fortuna and Tretiach (2018), the long-term radial growth of *X. parietina* varies according to climatic factors, and in dry climates, as in the Riotinto area, the growth ranges in the low end with approximately 1.27 mm during a period of 400 days.

2.2. Sample treatment and analysis

All the sample treatment and chemical analyses were performed at the Andalusian Institute of Earth Sciences (IACT, Granada, Spain) unless mentioned otherwise. The lichen samples were dried at 50 °C overnight, cleaned from debris such as remains of insects, ground and homogenized to obtain a fine powder. The dried samples were weighed (50.0 mg) into a pre-cleaned Teflon vial and subjected to acid digestion. The acids were previously distilled using a sub boiling system (Savillex). The digestion protocol consisted of adding 2 mL of purified HNO_3 (65% 14 M) and 0.25 mL of HF (24 M) under a metal-free ISO-100 vertical laminar flow hood in the cleanroom laboratory of Andalchron. The mixture was placed in Parr pressure reactors and heated in an oven at 150 °C during 20 h. The solution was then let to cool down, pipetted to Savillex vials, evaporated to complete dryness on a hot plate at 55 °C. To disintegrate any remaining organic compounds, 0.2 mL of H_2O_2 (30%) and 1 mL of purified HNO_3 (65% 14 M) were added, the vials were sealed and heated at 60 °C for 1 h and after cooling the solution was brought back to dryness (55 °C) and finally into solution by adding 1 mL purified HNO_3 (65% 14 M) and diluted for analysis. The final dilution for samples was 500x. The trace element concentration analyses (Sc, V, Cr, Mn, Co, Ni, Cu, Zn, As, Rb, Sr, Mo, Cd, Sn, Sb, Cs, Ba, W, Tl, Pb, Th, U) were performed on an Inductively Coupled Plasma Mass Spectrometer (ICP-MS, ThermoFinnigan iCap QR) at the analytical services Andalchron at the IACT. The matrix-matched reference materials IAEA-366 by the International Atomic Energy Agency, BCR-482 by the European Commission, and the rock RM W2-a (as also previously used by Rosca et al. (2019, 2018) for peat samples) were used as calibrators to deconvolute the element content of the samples. Major element concentrations (Na, K, Ca, Mg, S, Al, Fe) were determined by means of Inductively Coupled Plasma Optical Emission Spectrometry (ICP-OES, AVIO 500DV PerkinElmer) at the Department of Soil Sciences at the University of Granada, Spain. For quality assessment, chemical blanks and certified reference materials were ran along with the sample unknowns in the same measurement sessions. The results of the certified reference materials of IAEA-336 and BCR-482 are presented in the Supplementary Table S2, and the full results of the chemical analysis are given in Tables S3 and S4 for trace elements and major elements, respectively.

2.3. Statistical analysis

All statistical analyses were performed using IBM SPSS Statistics 21. The dataset was analyzed to verify the normal distribution of the elements, and as this was not fulfilled (with the exception of Th, K, Ca), hence, non-parametrical tests we used. Spearman's correlation was tested, and the *U* Mann Whitney test was run using the p value < 0.05 to determine whether the differences were considered significant between study and control areas. Kruskal Wallis was run to compare significant differences in the mean values between the towns of the study area, and additionally, ANOVA with Post Hoc Tukey test was run when the number of samples was insufficient for the previous test. Categorical Principal Component Analysis (CATPCA) was also run to simultaneously quantify categorical variables (towns in this case) while reducing the dimensionality of the dataset. The CATPCA was presented as a biplot.

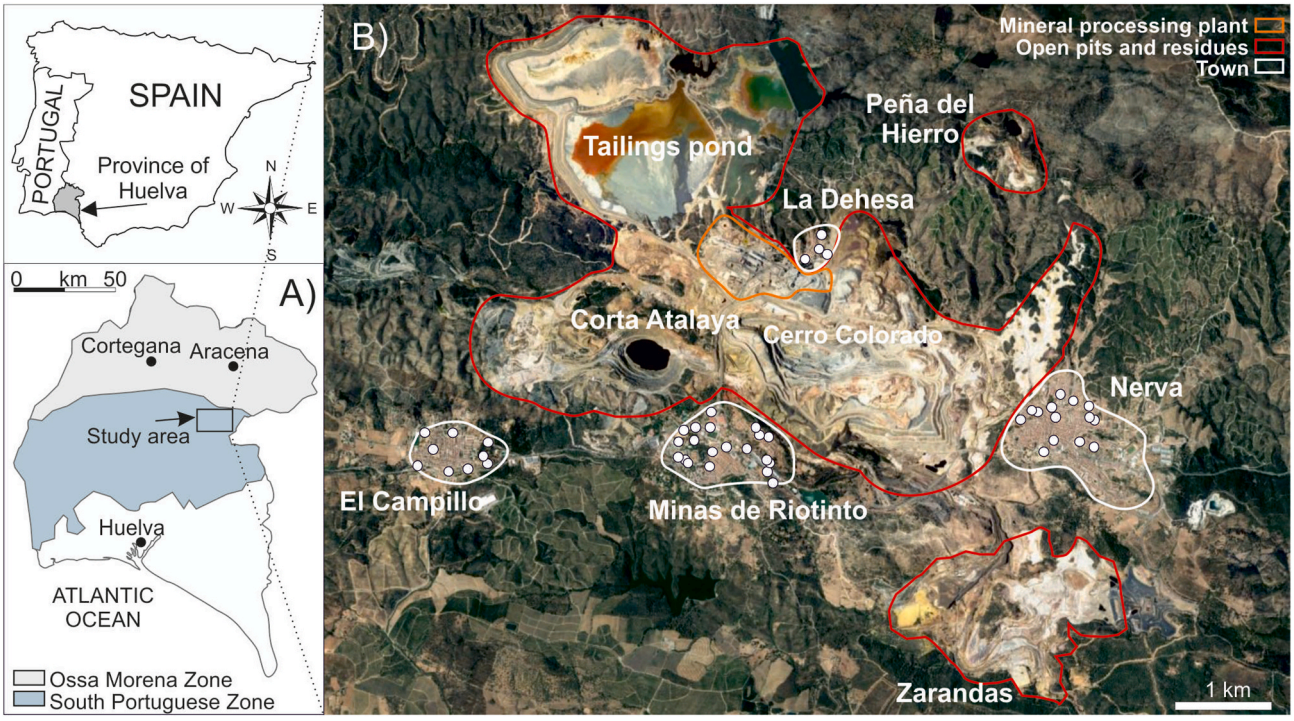

Fig. 1. A) A map of the geological units showing the study area and the control towns of Cortegana and Aracena, and B) a satellite image of study area in the Riotinto mining district and the sampling points in the towns of El Campillo, Minas de Riotinto, La Dehesa, and Nerva (Google Earth).

3. Results

3.1. Comparison of lichen samples in the study and control areas

Contrasting elemental abundances were observed between the study and control areas. The concentrations for Co, Ni, Cu, Zn, As, Rb, Mo, Cd, Sn, Sb, Cs, Ba, W, Tl, Pb, S, and Fe were higher in the study area in comparison to the control area, and the differences were statistically significant (Table 1). Only, the concentrations for Mn, Th, U, Na, and Ca were slightly higher in the control area with respect to study area, but the differences were significant only for U and Na. The highest trace element concentrations in the study area were measured for Cu (Max. 6181 mg/kg and mean 948 mg/kg), Zn (1412 mg/kg and 299 mg/kg), As (88 mg/kg and 22 mg/kg), Ba (438 mg/kg and 138 mg/kg), and Pb (267 mg/kg and 63 mg/kg) (Table 1). Furthermore, S and Fe exhibited high mean values (5465 and 8828 mg/kg, respectively). The kurtosis and standard deviation (Table 2) and Al-normalized data (Fig. S1) highlight the enrichment and greater dispersion of the PTEs in the study area in comparison to the control area. For instance, Ni, Cu, Zn, As, Mo, Sn, Sb, Tl, Pb, S, and Fe presented very little variation in the control areas, whereas the Al-normalized values ranged from similar values to up to >100 times higher values for lichens in the study area. Cadmium was an exception to the PTEs presenting higher dispersion in values in the control area. The concentrations of the PTEs of interest (Co, Ni, Cu, Zn, As, Rb, Mo, Cd, Sb, Cs, Ba, W, Tl, Pb, S, and Fe) in distal samples fell in between the values of the study and control areas (Table 1). One distal sample close to El Campillo exhibited high maximum values.

The Spearman's correlations exhibited, on the one hand, high positive intercorrelations (~0.75–0.90) between Co, Cu, Zn, As, Cd, Sn, Ba, Pb, S, and Fe (Table 2). On the other hand, V, Mn, Ni, Cs, and Al exhibited high positive intercorrelations (~0.70–0.89). Rubidium and Mo did not present correlations with any other elements, whereas Sr merely correlated with Ca (~0.70).

3.2. Spatial distribution of PTE pollution in the mining area

Fig. 2 exhibits the box plots of the elemental concentrations in lichens in all studied towns. The highest concentrations of all analyzed elements, except for Cr and Sr, correspond to the small settlement of La Dehesa located in the immediate vicinity of the mining plant and next to the tailings pond and the open pit of Cerro Colorado (Figs. 1 and 2). According to the ANOVA Tukey test (the non-parametric Kruskal Wallis test was not feasible due to the low number of samples in La Dehesa), the mean concentrations of Mn, Co, Cu, Zn, As, Sn, Sb, Ba, Pb, Mg, S, Al, and Fe were higher in La Dehesa with respect to the other towns in the study area. The mean concentrations of Cu and Pb were higher in Minas de Riotinto than in El Campillo and Nerva, but the differences were not statistically significant (Fig. 2). La Dehesa also stands out in the CATPCA (Cronbach's Alpha of 0.978), and similar trends of Minas de Riotinto and Nerva are suggested (Fig. 3). On the contrary, the distal samples exhibited similarities with the samples from Cortegana and Aracena. El Campillo fell in between the other towns of the study area and the control areas (Fig. 3). The first two components explained a total of 70.4% of the variance, where 52.4% corresponded to the first component and 18.0% to the second component. Cobalt, Cu, Zn, As, Cd, Sb, Ba, and Pb exhibited high saturation in the first component (0.75–0.93) and they were related to the samples in the study area. Furthermore, Supplementary Fig. S2 exhibits the spatial distribution of the elements of interest in the towns of El Campillo, Minas de Riotinto, La Dehesa, and Nerva. In Minas de Riotinto, the sampling points closest to the mining area had the highest concentrations, whereas clear trends in spatial distribution were not observed in El Campillo and in Nerva. However, Fig. S2 highlighted the great variation in the spatial distribution of PTEs within each town. As the results varied greatly in the study area within a radius of <5 km, these results implied the importance in choosing a representative monitoring site for atmospheric PM.

4. Discussion

4.1. Lichen and particulate matter characteristics and PTE sources in the study area

According to our investigation, the concentrations for Co, Ni, Cu, Zn, As, Rb, Mo, Cd, Sn, Sb, Cs, Ba, W, Tl, Pb, S, and Fe in lichens were statistically significantly higher in the study area in comparison to the control area, whereas Na and U were significantly higher in the control area with respect to the study area (Table 1). These differences owed to the characteristics of the geological context and to the PM composition in the atmosphere of each area (Fig. 1). Recent studies highlight As, Cu, Zn, Ba, and Pb as the main contaminants in the atmospheric PM in the towns of Minas de Riotinto, La Dehesa, and Nerva (Boente et al., 2022, 2023). According to Boente et al. (2023), La Dehesa shows higher concentrations of these elements in comparison to Minas de Riotinto and Nerva, especially during the warmest seasons. Our findings, based on 47 lichen bioindicator samples covering a larger area in the mining towns, are in accordance with the relative elemental abundances and distribution reported. These elements as well as Co, Cd, Sn, S, and Fe, presenting high positive intercorrelations in lichens are associated with the sulfide minerals of the ore deposit in the IPB (Table 2; Almodóvar et al., 2019; Sáez et al., 1999). The minerals of the ore deposit include pyrite [FeS_2], chalcopyrite [$CuFeS_2$], galena [PbS], sphalerite [ZnS], arsenopyrite [FeAsS], cobaltite [CoAsS], tetrahedrite–tennantite [$Cu_6(Cu_4X_2^{2+})Sb_4S_{13}$–$Cu_6(Cu_4X_2^{2+})As_4S_{13}$], Sb–As–Bi sulfosalts, as well as hematite [Fe_2O_3], magnetite [Fe_3O_4], cassiterite [SnO_2], and barite [$BaSO_4$] (Almodóvar et al., 2019). Another study reports mineralogical composition of PM collected in Nerva and highlights that primary sulfides (pyrite, chalcopyrite, galena, sphalerite, and bornite) and their oxidation products (goethite, hematite, and jarosite) are responsible for sulfide-associated elements in the PM (Fernández Caliani et al., 2013). These authors attribute the concentrations of As, Bi, Cd, Cu, Pb, Sb and Zn to the adjacent mine waste dumps. Arsenic, Cu, Zn, Ba, and Pb are also recognized as the main PTEs in urban soils of Minas de Riotinto (Parviainen et al., 2022b; Vázquez-Arias et al., 2023). The minerals in soils carrying these elements include primary sulfides and secondary minerals such as beudantite [$PbFe_3(AsO_4)(SO_4)(OH)_6$], arsenian plumbojarosite [$Pb_{0.59}Fe_3(AsO_4)_{0.18}(SO_4)_{1.82}(OH)_6$], and Fe(III)hydroxides (Parviainen et al., 2022b). The principal origin of the PTEs in urban soil is the natural soil forming processes developed from the adjacent bedrock that contains mineralizations in the proximities of the sulfide ore deposits of the IPB (Vázquez-Arias et al., 2023). These authors also acknowledge a minor input from the deposition of atmospheric PM over decades which can be observed in the old parks covered with calcareous aggregate pavements that are naturally PTE-poor. Other studies also corroborate elevated concentrations in topsoils surrounding El Campillo with maximum values encountered closer to the ore deposits and the abandoned open pit, including As (up to 2234 mg/kg), Cu (1119 mg/kg), Pb (3494 mg/kg), and Zn (723 mg/kg) (Zuluaga et al., 2017). These values are similar to the ones observed in the soils of Minas de Riotinto (Vázquez-Arias et al., 2023). Based on these observations, the local geochemical background levels both in the bedrock as well as in soils may influence the lichen composition with elevated concentrations of the main PTEs.

A further examination reveals that the mean elemental ratios of the main PTEs (Pb/As–Zn/Pb–Cu/Zn) for both lichen and PM samples present similar trends in the ternary plot (Fig. 4). Moreover, Boente et al. (2022) divide the PM samples into two clusters in their ternary plot of Cu/As–Zn/Pb–Cu/Zn where Nerva and Minas de Riotinto present similar elemental ratios with PM from most of the mining operations that they studied, whereas La Dehesa presents similar ratios with PM derived from wet ore loading, a ceased stockpile, and tailings pond dry track in close vicinity to the settlement (figs. 5 and 6 in Boente et al., 2022). In Fig. 4 we presented the clusters defined by Boente et al. (2022) along with our results to be able to compare their results with ours. This

Table 1
Min., max., mean, and median concentrations (mg/kg), standard deviation (SD) and kurtosis for lichen samples in the study (n = 47), control areas (n = 33), and distal samples (n = 9). The values in bold indicate statistically significantly higher mean concentrations in the study area with respect to control area according to the *U* Mann Withey test. (<DL = Below detection limit).

	Study area						Control area						Distal samples					
	Min.	Max.	Mean	Median	SD	Kurtosis	Min.	Max.	Mean	Median	SD	Kurtosis	Min.	Max.	Mean	Median	SD	Kurtosis
Sc	0.54	4.0	1.5	1.3	0.81	1.43	0.58	2.3	1.2	1.0	0.52	−0.88	0.67	2.6	1.4	1.3	0.56	1.69
V	5.6	49	16	13	9.3	4.77	5.8	30	13	11	5.6	2.18	5.6	23	14	13	5.1	0.71
Cr	7.2	67	18	16	10	11.0	5.6	45	14	12	7.8	6.22	4.9	46	18	16	12	2.81
Mn	59	492	189	167	103	1.72	66	487	230	190	127	−0.76	69	897	368	241	315	−0.50
Co	1.4	12	**4.1**	**3.1**	2.5	2.96	0.70	2.5	1.4	1.3	0.45	0.004	0.70	2.6	1.6	1.5	0.55	0.81
Ni	2.4	14	**6.2**	**5.6**	2.5	1.51	2.3	9.4	4.5	4.1	1.7	1.11	2	12	6.4	6.7	2.8	1.22
Cu	87	6181	**948**	**489**	1265	6.59	17	108	41	35	21	2.81	26	1074	177	63	338	8.78
Zn	70	1412	**299**	**178**	320	4.32	33	228	91	76	45	2.50	46	173	116	113	46	−1.40
As	6.3	88	**22**	**18**	16	6.80	1.2	5.5	2.7	2.1	1.2	−0.09	2.6	9	4.4	3.3	2.4	0.65
Rb	11	46	**19**	**18**	6.1	6.80	8.0	31	16	16	6.3	−0.25	6.6	29	18	16	7.5	−0.50
Sr	9.9	119	24	21	16	29.7	10	35	20	19	5.7	0.34	14	41	22	21	8.5	2.29
Mo	0.82	13	**2.9**	**2.0**	2.5	6.07	0.25	4.3	0.96	0.72	0.90	7.28	0.58	2.2	1.1	0.87	0.61	−0.60
Cd	0.090	1.1	**0.29**	**0.20**	0.21	5.01	0.04	0.62	0.13	0.082	0.15	5.16	0.033	0.76	0.18	0.11	0.22	7.18
Sn	1.9	31	**6.4**	**4.6**	6.2	8.44	0.59	4.6	1.8	1.5	0.99	2.26	0.63	6.1	2.2	1.8	1.8	2.09
Sb	0.00	97	**12**	**4.8**	20	7.47	0.47	3.6	1.3	1.2	0.69	3.13	0.40	6.3	1.8	1.2	1.8	5.26
Cs	0.32	1.3	**0.66**	**0.64**	0.24	0.25	0.28	1.9	0.58	0.53	0.30	12.1	0.25	1.7	0.73	0.60	0.45	1.78
Ba	42	438	**138**	**123**	84	3.84	30	145	74	63	31	−0.21	23	153	67	60	36	5.00
W	0.090	0.45	**0.23**	**0.25**	0.086	0.44	0.090	0.35	0.17	0.16	0.070	0.17	0.10	0.31	0.18	0.16	0.069	0.65
Tl	0.090	0.37	**0.19**	**0.18**	0.080	0.15	0.030	0.27	0.10	0.082	0.047	4.23	0.030	0.12	0.079	0.087	0.027	0.24
Pb	13	267	**63**	**34**	69	2.95	5.2	38	14	11	8.0	1.24	4.4	29	13	10	8.6	0.43
Th	0.22	0.96	0.52	0.49	0.20	−0.74	0.23	1.3	0.54	0.48	0.25	2.59	0.21	0.82	0.48	0.53	0.18	0.28
U	0.080	0.32	0.19	0.18	0.055	0.13	0.11	0.57	**0.24**	**0.21**	0.10	2.00	0.070	0.27	0.15	0.14	0.056	1.81
Na	252	2275	732	586	414	2.95	418	3431	**966**	**875**	555	11.6	477	1182	721	677	196	4.31
K	5667	10208	7606	7553	1109	−0.16	5463	8435	7237	7302	681	0.11	4509	6986	5625	5481	906	−1.40
Ca	1578	7180	4061	3852	1272	−0.30	2959	10881	4781	4458	1699	4.76	2238	5801	4002	3297	1446	−2.10
Mg	674	8120	2665	2131	1595	3.90	957	3633	2243	2211	619	0.32	<DL	4241	2024	2328	1344	−0.65
S	2426	13848	**5465**	**4749**	2529	4.26	1932	3817	2746	2703	428	0.036	1941	4108	3374	3405	695	1.10
Al	2791	22308	8450	4749	4543	1.43	3314	15109	6696	5893	2726	1.42	3267	9731	7107	8117	2433	−0.92
Fe	2406	37980	**8828**	**6518**	7882	6.43	2216	8536	4623	3893	1813	−0.62	1953	6730	4294	4790	1506	−0.30

Table 2
Spearman's correlation for lichen samples in the study area. High positive correlations (>0.70) are indicated in bold.

	Sc	V	Cr	Mn	Co	Ni	Cu	Zn	As	Rb	Sr	Mo	Cd	Sn	Sb	Cs	Ba	W	Tl	Pb	Th	U	Na	K	Ca	Mg	S	Al	Fe
Sc	1.00	**0.72**	0.54	0.61	0.66	0.62	0.60	0.63	0.38	0.41	0.50	0.03	0.60	0.60	0.43	0.58	0.62	0.69	0.41	0.59	**0.85**	**0.74**	0.56	−0.11	0.51	0.60	0.50	**0.80**	**0.74**
V		1.00	**0.83**	**0.76**	0.67	**0.84**	0.53	0.58	0.31	0.43	0.49	−0.10	0.61	0.63	0.08	**0.89**	0.56	0.53	0.22	0.35	0.54	**0.70**	**0.75**	0.19	0.28	0.68	0.48	**0.86**	0.66
Cr			1.00	0.52	0.52	**0.77**	0.43	0.42	0.19	0.32	0.39	−0.01	0.52	0.54	−0.05	**0.70**	0.41	0.47	0.17	0.26	0.40	0.61	**0.78**	0.34	0.18	0.52	0.35	0.66	0.55
Mn				1.00	**0.77**	0.65	0.58	**0.78**	0.56	0.44	0.31	−0.12	**0.75**	0.62	0.02	**0.80**	0.63	0.39	0.32	0.39	0.37	0.49	0.40	0.25	0.23	**0.77**	0.68	**0.78**	0.68
Co					1.00	0.62	**0.83**	**0.88**	**0.80**	0.40	0.29	0.14	**0.77**	**0.82**	0.27	0.59	**0.81**	0.54	0.56	**0.71**	0.42	0.40	0.30	0.17	0.27	**0.74**	**0.85**	**0.70**	**0.90**
Ni						1.00	0.49	0.56	0.28	0.28	0.55	−0.04	0.63	0.58	0.01	**0.80**	0.47	0.42	0.19	0.28	0.43	0.60	0.63	0.24	0.39	0.57	0.42	**0.70**	0.58
Cu							1.00	**0.83**	0.65	0.37	0.07	0.23	**0.77**	**0.78**	0.49	0.42	0.68	0.60	0.68	**0.72**	0.45	0.39	0.35	0.09	0.25	**0.76**	**0.79**	0.68	**0.86**
Zn								1.00	0.68	0.32	0.26	−0.01	**0.91**	**0.73**	0.27	0.51	**0.75**	0.51	0.53	0.63	0.44	0.42	0.31	0.16	0.32	**0.70**	**0.77**	0.67	**0.82**
As									1.00	0.31	−0.07	0.15	0.54	**0.77**	0.25	0.30	**0.81**	0.39	**0.71**	**0.79**	0.19	0.14	−0.08	−0.03	−0.04	0.51	**0.77**	0.41	**0.75**
Rb										1.00	0.03	0.09	0.39	0.43	0.39	0.46	0.48	0.52	0.37	0.41	0.36	0.44	0.33	0.08	0.18	0.58	0.29	0.53	0.47
Sr											1.00	−0.24	0.35	0.15	−0.16	0.42	0.20	0.26	−0.13	0.05	0.45	0.41	0.38	0.16	**0.70**	0.24	0.09	0.37	0.25
Mo												1.00	−0.08	0.18	0.33	−0.09	0.03	0.27	0.26	0.26	0.11	−0.01	0.01	−0.05	−0.07	0.14	0.35	0.07	0.23
Cd													1.00	0.68	0.17	0.58	0.66	0.49	0.48	0.54	0.42	0.44	0.40	0.23	0.41	**0.71**	0.64	0.67	**0.75**
Sn														1.00	0.32	0.55	**0.81**	0.64	0.69	**0.79**	0.46	0.49	0.41	0.03	0.18	0.69	**0.73**	**0.71**	**0.88**
Sb															1.00	−0.07	0.25	0.56	0.49	0.58	0.47	0.31	0.17	−0.28	0.10	0.30	0.20	0.36	0.43
Cs																1.00	0.52	0.41	0.19	0.24	0.43	0.58	0.61	0.19	0.25	0.65	0.49	**0.78**	0.56
Ba																	1.00	0.59	0.70	**0.79**	0.49	0.47	0.28	0.00	0.22	0.63	**0.72**	0.66	**0.83**
W																		1.00	0.60	**0.76**	**0.84**	**0.81**	0.62	−0.09	0.34	0.64	0.48	**0.79**	**0.79**
Tl																			1.00	**0.81**	0.42	0.34	0.15	−0.14	0.06	0.48	0.57	0.44	0.68
Pb																				1.00	0.58	0.44	0.26	−0.24	0.23	0.56	0.64	0.59	**0.88**
Th																					1.00	0.87	0.65	−0.19	0.48	0.48	0.33	**0.75**	0.63
U																						1.00	0.81	0.04	0.34	0.55	0.28	**0.82**	0.58
Na																							1.00	0.18	0.33	0.49	0.18	**0.75**	0.47
K																								1.00	0.01	0.29	0.27	0.07	−0.02
Ca																									1.00	0.33	0.15	0.35	0.33
Mg																										1.00	**0.74**	**0.82**	**0.80**
S																											1.00	0.60	**0.79**
Al																												1.00	**0.83**
Fe																													1.00

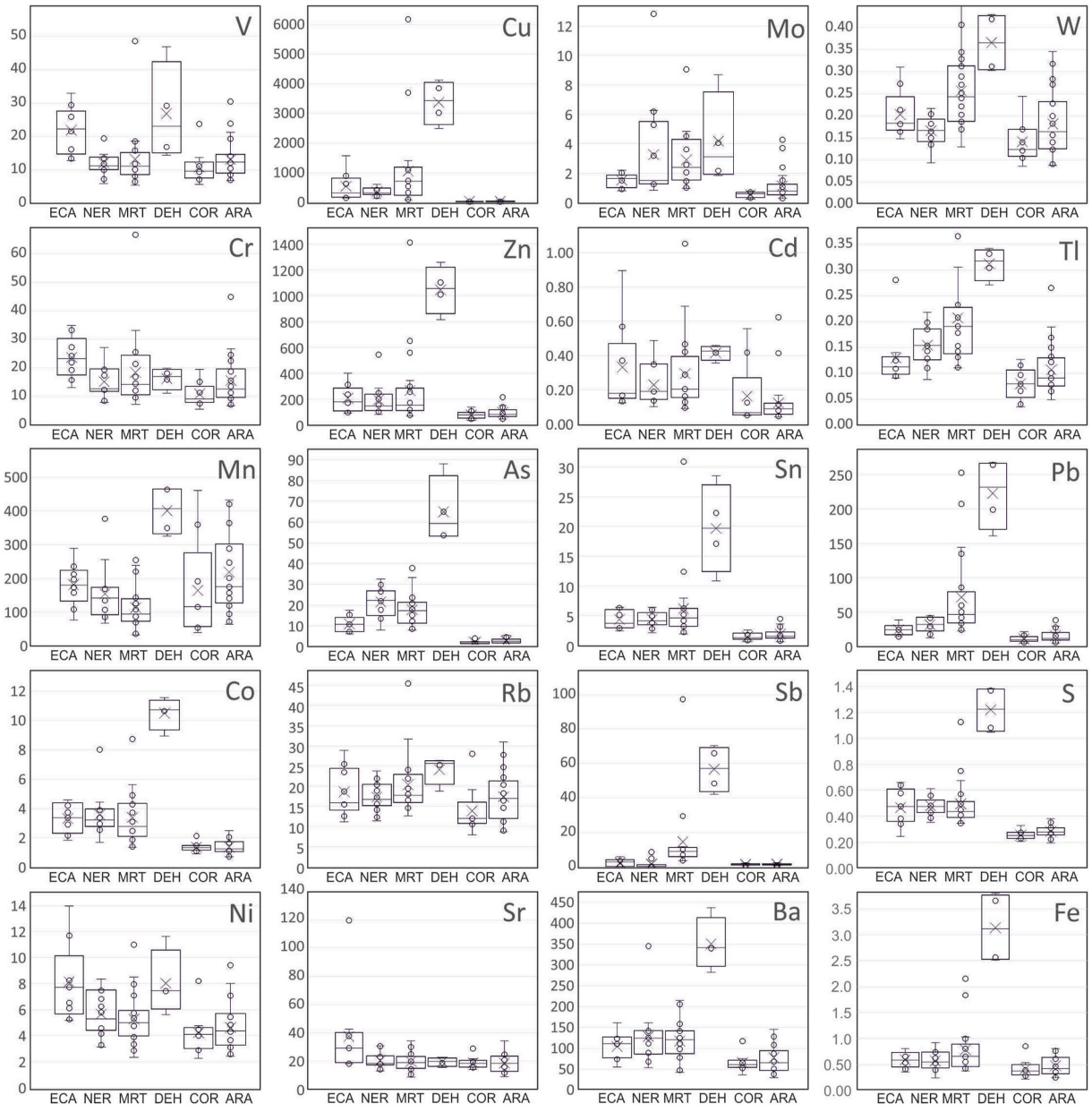

Fig. 2. Box plots presenting the concentrations of the main PTEs (values in mg/kg, except for S and Fe in Wt.%). Samples from the study area: ECA = El Campillo, NER = Nerva, MRT = Minas de Riotinto, DEH = La Dehesa; and samples from control area: COR = Cortegana, ARA = Aracena.

Figure presents also the data for the Spanish town of Granada where the main pollution source is traffic (Parviainen et al., 2020) as well as the town of Huelva where industrial activity, especially a Cu smelter, contributes to the main pollution source (Parviainen et al., 2019). In the Cu/As–Zn/Pb–Cu/Zn ternary plot we were unable to discriminate the traffic source, therefore instead we plotted Pb/As–Zn/Pb–Cu/Zn plot that highlighted the different clustering of the lichen samples collected from Granada in comparison to the study area (Fig. 4). The Pb/As ratios were much higher in the town of Granada (representing completely different geochemical background and traffic as the main source of PTEs) with respect to the areas with sulfur mineralizations and industrial activity related to mining including the study area and the town of Huelva. The elemental ratios of the lichen samples from Huelva presented a similar elemental ratio with the cluster 2 which may be explained by the similar sulfur mineral origin. One must bear in mind that the lichens collected in this study (peripheral part of native lichens) reflect the atmospheric state over a period of the past <4 years. The Pb/As–Zn/Pb–Cu/Zn ternary plot shows different trends between lichen samples from the control and study areas, although the lichen samples from Cortegana and Aracena present similar values to the PM samples of the cluster 1 (Boente et al., 2022). The similar elemental ratios of lichen samples from Aracena and the study area may be explained by adjacent supergene alteration of a primary carbonate-hosted sphalerite and galena mineralization and subsequent concentrations of the released trace elements in the soil (Rivera et al., 2015; Vázquez-Arias et al., 2023). These mineralizations affected the soil chemistry in the Aracena area. However, lichens in Aracena contained significantly lower concentrations of Cu, Zn, As and Pb than in the study towns, yet the elemental ratios seemed to reflect the geochemical signature of sulfide mineralizations and local soils.

During the period when the mining activity ceased (2009–2014), the concentrations of PTEs in PM in Nerva were lower (mean concentration of 1.1 ng/m^3 for As, 6.1 ng/m^3 for Cu, 23 ng/m^3 for Zn, and 4.8 ng/m^3 for Pb; Sánchez de la Campa et al., 2020) than during the mining activity in 2018 (1.8 ng/m^3 for As, 15 ng/m^3 for Cu, 28 ng/m^3 for Zn, and 5.7 ng/m^3 for Pb; Boente et al., 2022). The PTE levels in the dust derived

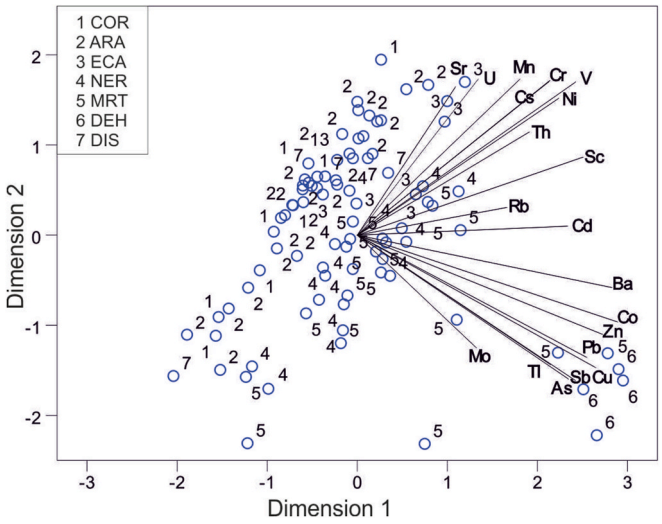

Fig. 3. Categorical PCA biplot for lichen samples from Cortegana (1 = COR), Aracena (2 = ARA), El Campillo (3 = ECA), Nerva (4 = NER), Minas de Riotinto (5 = MRT), and La Dehesa (6 = DEH). Distal samples (7 = DIS) are also presented.

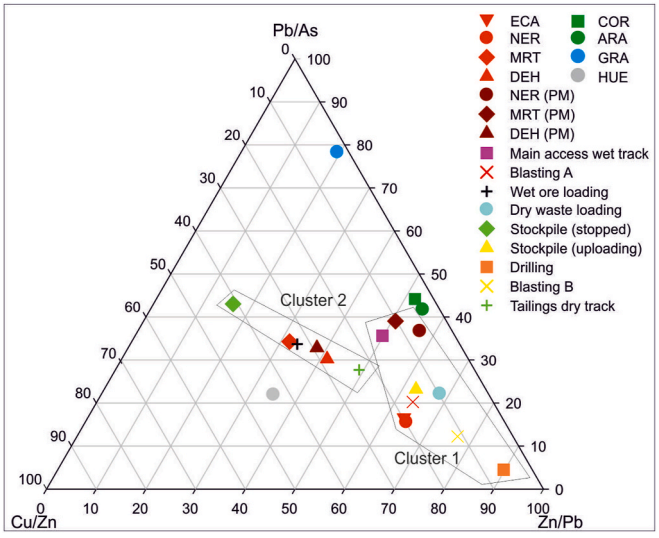

Fig. 4. Mean elemental ratios presented in a Pb/As–Zn/Pb–Cu/Zn ternary plot for lichen samples in the towns of the study area including El Campillo (ECA), Nerva (NER), Minas de Riotinto (MRT), and La Dehesa (DEH) and in the control towns of Cortegana (COR) and Aracena (ARA), as well as in Granada (GRA; Parviainen et al., 2020) and Huelva (HUE; Parviainen et al., 2019). PM samples of the study area and the mine workings are also presented (modified from Boente et al., 2022).

from various types of mining operations are much higher than the PM gauged in the monitoring stations in the nearby towns. For example, the tailings pond track exhibited the highest concentrations among the different mining operations (229 ng/m^3 for As, 4842 ng/m^3 for Cu, 2382 ng/m^3 for Zn, and 555 ng/m^3 for Pb) (Boente et al., 2022). The atmospheric PM derived from the mining activities experiences a rapid dilution effect in the air. One km distance from the mine in Minas de Riotinto or two km distance in Nerva, the concentrations decrease substantially (Boente et al., 2022). The distal lichen samples corroborate the dilution effect in the atmosphere especially after 5 km, and in this study, we recorded similar mean concentrations for As (4.4 mg/kg) and Pb (13 mg/kg) in the distal samples as in the samples from the control areas. Copper (177 mg/kg) and Zn (116 mg/kg) exhibited much lower concentrations in the distal samples than in the study areas, but higher than in the control areas. These elevated mean values are affected by one distal sample 5 km to the west from the mining area, close to El Campillo. In the field, we observed mineralized bedrock outcrops that may have influenced the chemical composition of the lichens.

According to the human health risk assessment based on the PM levels in 2021, the elemental concentrations do not surpass the regulatory limits of the cumulative hazard index (HI = 1) in any of the towns, but in La Dehesa the HI is 0.9 with As accounting for more than half of the contribution of the overall non-carcinogenic risk (Boente et al., 2023). Therefore, monitoring the pollution levels in La Dehesa is recommended (Boente et al., 2023). Considering the high concentrations of PM produced by the mining operations (drilling, blasting, transportation, stockpiling, etc.), the mine workers, depending on their tasks, may be at higher exposure risk. According to our study, lichens exhibited extreme accumulation of PTEs especially in the urban areas of Minas de Riotinto and La Dehesa. These data support the recommendation of monitoring the pollution levels in these towns. In addition to the atmospheric pollution, urban soils —in many cases exceeding the regulatory values for As and Pb (p. 28-64)— have been suggested to contribute to the potential human health risk of the residents in the Riotinto mining district. In a previous study, the urban soils of Minas de Riotinto were considered as an exposure area, and the soils presented increased carcinogenic risk for both children and adults (Parviainen et al., 2022a).

4.2. Comparison to PTE levels in other sites

The maximum concentrations of Cu, Zn, As, Ba, and Pb in lichens in the mining district of Riotinto exhibit extreme values with the highest values corresponding to sampling locations in La Dehesa (Table 1 and Fig. 2). The mean values of these elements (Cu 948 mg/kg, Zn 299 mg/kg, As 22 mg/kg, Ba 138 mg/kg, and Pb 63, respectively) were elevated in comparison to other areas affected by industrial activities related to mining. For example, in the city of Huelva, under the impact of a Cu smelter and other industrial activities, elevated mean values of Cu (769 mg/kg), Zn (138 mg/kg), As (11 mg/kg), Ba (54 mg/kg), and Pb (31 mg/kg) have been documented in *X. parietina* (Parviainen et al., 2019). These values are also very high, but they represent lower pollution levels than observed in this study. In Slovakia, nearby a slag heap of a former Ni smelter, concentrations of Ni (150 mg/kg) are elevated in *X. parietina*, whereas other PTEs of interest have lower values including Cu (8.3 mg/kg), Zn (36 mg/kg), Ba (20 mg/kg), Pb (1.4 mg/kg), and As (1.9 mg/kg) (Kováčik et al., 2023). In the surroundings of the Sudbury smelter 31 mg/kg of Pb was measured in *Cladonia rangiferina* (2 km from the source) (Widory et al., 2018). These examples show different concentrations than those found in Riotinto, since they are developed in different mineralogical contexts; however, they reveal the key role of lichens as indicators of environmental importance.

When comparing the study area with other urban areas in Spain that are not under the influence of mining activities, the values in El Campillo, Minas de Riotinto, Nerva and La Dehesa, stand out with extreme values. In Granada, a non-industrialized Spanish city, where traffic is the main source of air pollution, the mean values for Cu, Zn, As, Ba, and Pb in *X. parietina* are much lower (24 mg/kg, 63 mg/kg, 1.6 mg/kg, 46 mg/kg, and 20 mg/kg, respectively; Parviainen et al., 2020). These values remain even below the mean concentrations that were gauged in the lichens from the control populations of Cortegana and Aracena except for Pb (Table 1).

5. Conclusions

This study establishes the trace metal distribution patterns in the atmosphere in the urban areas of the mining district of Riotinto (SW Spain) using lichens as bioindicators, and highlights Cu, Zn, As, Ba, and Pb as the most relevant potential pollutants. These PTEs presenting

extreme values are associated with the main ore minerals of the massive sulfide deposits of the IPB. These and other sulfide-associated PTEs, including Co, Ni, Mo, Cd, Sn, Sb, Tl, S, and Fe, exhibit significantly higher values in the study area, encompassing towns of El Campillo, Minas de Riotinto, Nerva, and La Dehesa, in comparison to the control area out of the immediate reach of mining (Cortegana and Aracena).

The highest PTE concentrations are found in the settlement of La Dehesa in close vicinity to the mining activities, especially with the mineral processing plant and the tailings pond. The other three towns, one to two km distance from the mine workings, exhibit slight differences in the spatial distribution of the PTEs in lichens, and the distal samples highlight that the atmospheric pollution derived from the massive sulfide deposits experiences a rapid dilution effect. The concentrations of the distal samples decrease to values comparable to control areas after 5 km distance from Riotinto. Thereby, the lichen bioindicators prove the dispersion of sulfide-associated PTEs in the surroundings of the mine workings and the impact on the nearby urban areas. Based on elemental ratios in lichens, this study also distinguishes the sulfide-related source from traffic source. Furthermore, the extreme concentrations of As, Cu, Zn, and Pb in the study area are an indication of potential chronic human exposure via inhalation and potential health risks on the long run. Therefore, monitoring of the air quality is recommended.

CRediT authorship contribution statement

Annika Parviainen: Writing – original draft, Methodology, Investigation, Funding acquisition, Formal analysis, Conceptualization. **Carolina Rosca:** Writing – review & editing, Methodology. **Deyanira Rondon:** Writing – review & editing, Methodology. **Manuel Casares Porcel:** Writing – review & editing. **Francisco José Martín-Peinado:** Writing – review & editing, Conceptualization.

Declaration of competing interest

The authors declare the following financial interests/personal relationships which may be considered as potential competing interests: Annika Parviainen reports financial support was provided by University of Granada. Annika Parviainen reports financial support was provided by Government of Andalusia. If there are other authors, they declare that they have no known competing financial interests or personal relationships that could have appeared to influence the work reported in this paper.

Data availability

Data is available in the Supplementary Tables S3 and S4. in the Supplemental Material

Acknowledgements

We acknowledge Mrs. María del Carmen Carrasco Sierra and Mr. M. J. Roman Alpiste for their assistance in laboratory work for chemical analyses. This work was supported by the BIMESUS project (E-RNM-422-UGR20) funded by the University of Granada (Spain) and by the IMAGE project (EMC21_00056) granted by the Council of University, Research and Innovation of the Regional Government of Andalusia (Spain). Funding for open access charge: University of Granada / CBUA. Dr. Deyanira Rondón thanks grant PTA2019-016727-I funded by MICIU/AEI/10.13039/501100011033 and Dr. Carolina Rosca thanks grant PTA2022-021985-I funded by MICIU/AEI/10.13039/501100011033 and by FSE+.

Appendix A. Supplementary data

Supplementary data to this article can be found online at https://doi.org/10.1016/j.chemosphere.2024.142906.

References

Almodóvar, G.R., Yesares, L., Sáez, R., Toscano, M., González, F., Pons, J.M., 2019. Massive sulfide ores in the iberian pyrite belt: mineralogical and textural evolution. Minerals 9. https://doi.org/10.3390/min9110653.

Andalusian Institute of Statistics and Cartography, 2022. URL. https://www.juntadeandalucia.es/institutodeestadisticaycartografia/temas/est/tema_poblacion-en.htm.

Atalaya Minining, 2023. Preliminary Economic Assessment. Riotinto District [WWW Document] 166. https://wp-atalaya-mining-2022.s3.eu-west-2.amazonaws.com/media/2023/03/2023.02.21-ATYM-Riotinto-NI-43-101-Technical-Report-PEA-vF.pdf.

Bari, A., Rosso, A., Minciardi, M.R., Troiani, F., Piervittori, R., 2000. Analysis of heavy metals in atmospheric particulates in relation to their bioaccumulation in explanted Pseudevernia furfuracea thalli. Environ. Monit. Assess. 205–220.

Boente, C., Millán-Martínez, M., Sánchez de la Campa, A.M., Sánchez-Rodas, D., de la Rosa, J.D., 2022. Physicochemical assessment of atmospheric particulate matter emissions during open-pit mining operations in a massive sulphide ore exploitation. Atmos. Pollut. Res. 13 https://doi.org/10.1016/j.apr.2022.101391.

Boente, C., Zafra-Pérez, A., Fernández-Caliani, J.C., Sánchez de la Campa, A., Sánchez-Rodas, D., de la Rosa, J.D., 2023. Source apportionment of potentially toxic PM10 near a vast metallic ore mine and health risk assessment for residents exposed. Atmos. Environ. 301 https://doi.org/10.1016/j.atmosenv.2023.119696.

Branquinho, C., 2001. Lichens. In: Metals in the Environment. CRC Press, pp. 137–178.

Cecconi, E., Fortuna, L., Benesperi, R., Bianchi, E., Brunialti, G., Contardo, T., Nuzzo, L. Di, Frati, L., Monaci, F., Munzi, S., Nascimbene, J., Paoli, L., Ravera, S., Vannini, A., Giordani, P., Loppi, S., Tretiach, M., 2019. New interpretative scales for lichen bioaccumulation data: the Italian proposal. Atmosphere 10, 1–19. https://doi.org/10.3390/atmos10030136.

Conti, M.E., Cecchetti, G., 2001. Biological monitoring: lichens as bioindicators of air pollution assessment - a review. Environ. Pollut. 114, 471–492. https://doi.org/10.1016/S0269-7491(00)00224-4.

Decree 18. Decreto 18/2015, de 27 de enero, por el que se aprueba el reglamento que regula el régimen aplicable a los suelos contaminados (Decree 18/2015, on 27th of January 2015, approving the regulation that regulates the regime applicable for contaminated soils. Junta de Andalucía. https://www.juntadeandalucia.es/boja/2015/38/3.

Fernández Caliani, J.C., Rosa Díaz, J., Sánchez de la Campa Verdona, A.M., González Castanedo, Y., Castillo, S., 2013. Mineralogy of atmospheric dust impacting the Rio Tinto mining area (Spain) during episodes of high metal deposition. Mineral. Mag. 77, 2793. https://doi.org/10.1180/minmag.2013.077.6.07.

Fortuna, L., Tretiach, M., 2018. Effects of site-specific climatic conditions on the radial growth of the lichen biomonitor Xanthoria parietina. Environ. Sci. Pollut. Res. 25, 34017–34026. https://doi.org/10.1007/s11356-018-3155-z.

Francová, A., Chrastný, V., Šillerová, H., Vítková, M., Kocourková, J., Komárek, M., 2017. Evaluating the suitability of different environmental samples for tracing atmospheric pollution in industrial areas. Environ. Pollut. 220, 286–297. https://doi.org/10.1016/j.envpol.2016.09.062.

Jiménez-Moreno, M., Barre, J.P.G., Perrot, V., Bérail, S., Rodríguez Martín-Doimeadios, R.C., Amouroux, D., 2016. Sources and fate of mercury pollution in Almadén mining district (Spain): evidences from mercury isotopic compositions in sediments and lichens. Chemosphere 147, 430–438. https://doi.org/10.1016/j.chemosphere.2015.12.094.

Knops, J.M.H., Iii, T.H.N., Boucher, V.L., Schlesinger, W.H., 1991. Mineral cycling and epiphytic lichens: implications at the ecosystem level. Lichenol. 23, 309–321. https://doi.org/10.1017/S0024282991000452.

Kováčik, J., Husáková, L., Vlassa, M., Piroutková, M., Vydra, M., Patočka, J., Filip, M., 2023. Elemental profile identifies metallurgical pollution in epiphytic lichen Xanthoria parietina and (hypo)xanthine correlates with metals. Sci. Total Environ. 883 https://doi.org/10.1016/j.scitotenv.2023.163527.

Nieto, J.M., Sarmiento, A.M., Canovas, C.R., Olias, M., Ayora, C., 2013. Acid mine drainage in the Iberian Pyrite Belt: 1. Hydrochemical characteristics and pollutant load of the Tinto and Odiel rivers. Environ. Sci. Pollut. Res. https://doi.org/10.1007/s11356-013-1634-9.

Nocete, F., Sáez, R., Bayona, M.R., Nieto, J.M., Peramo, A., López, P., Gil-Ibarguchi, J.I., Inácio, N., García, S., Rodríguez, J., 2014. Gold in the southwest of the iberian peninsula during the 3rd millennium BC. J. Archaeol. Sci. https://doi.org/10.1016/j.jas.2013.10.006.

OECD, 2019. Global Material Resources Outlook to 2060: Economic Drivers and Environmental Consequences. https://doi.org/10.1787/9789264307452-en. Paris.

Parviainen, A., Casares-Porcel, M., Marchesi, C., Garrido, C.J., 2019. Lichens as a spatial record of metal air pollution in the industrialized city of Huelva (SW Spain). Environ. Pollut. 253, 918–929. https://doi.org/10.1016/j.envpol.2019.07.086.

Parviainen, A., Papaslioti, E.M., Casares-Porcel, M., Garrido, C.J., 2020. Antimony as a tracer of non-exhaust traffic emissions in air pollution in Granada (S Spain) using lichen bioindicators. Environ. Pollut. 263 https://doi.org/10.1016/j.envpol.2020.114482.

Parviainen, A., Vázquez-Arias, A., Arrebola-Moreno, J.P., Martín-Peinado, F.J., 2022a. Human health risks associated with urban soils in mining areas. Environ. Res. 206, 112514 https://doi.org/10.1016/j.envres.2021.112514.

Parviainen, A., Vázquez-Arias, A., Martín-Peinado, F.J., 2022b. Mineralogical association and geochemistry of potentially toxic elements in urban soils under the influence of mining. Catena 217, 106517. https://doi.org/10.2139/ssrn.4111903.

Rasmussen, H.N., Nord-Larsen, T., Hansen, E.S., Hoareau, G., 2018. Estimation of life history in corticolous lichens by zonation. Lichenologist 50, 697–704. https://doi.org/10.1017/S0024282918000440.

Rivera, M.B., Fernández-Caliani, J.C., Giráldez, M.I., 2015. Geoavailability of lithogenic trace elements of environmental concern and supergene enrichment in soils of the Sierra de Aracena Natural Park (SW Spain). Geoderma 259–260, 164–173. https://doi.org/10.1016/j.geoderma.2015.06.009.

Rosca, C., Schoenberg, R., Tomlinson, E.L., Kamber, B.S., 2019. Combined zinc-lead isotope and trace-metal assessment of recent atmospheric pollution sources recorded in Irish peatlands. Sci. Total Environ. 658, 234–249. https://doi.org/10.1016/j.scitotenv.2018.12.049.

Rosca, C., Tomlinson, E.L., Geibert, W., McKenna, C.A., Babechuk, M.G., Kamber, B.S., 2018. Trace element and Pb isotope fingerprinting of atmospheric pollution sources: a case study from the east coast of Ireland. Appl. Geochem. 96, 302–326. https://doi.org/10.1016/j.apgeochem.2018.07.003.

Ruiz de Almodóvar Sel, G., Pérez López, R., 2008. Recursos minerales. In: Manuel, O.Á. (Ed.), Universidad de Huelva, Huelva, pp. 37–43.

Sáez, R., Pascual, E., Toscano, M., Almodóvar, G.R., 1999. The Iberian type of volcano-sedimentary massive sulphide deposits. Miner. Depos. 34, 549–570. https://doi.org/10.1007/s001260050220.

Saib, H., Yekkour, A., Toumi, M., Guedioura, B., Benamar, M.A., Zeghdaoui, A., Austruy, A., Bergé-Lefranc, D., Culcasi, M., Pietri, S., 2023. Lichen biomonitoring of airborne trace elements in the industrial-urbanized area of eastern algiers (Algeria). Atmos. Pollut. Res. 14 https://doi.org/10.1016/j.apr.2022.101643.

Sánchez de la Campa, A.M., Sánchez-Rodas, D., Márquez, G., Romero, E., de la Rosa, J. D., 2020. 2009–2017 trends of PM10 in the legendary Riotinto mining district of SW Spain. Atmos. Res. 238, 104878 https://doi.org/10.1016/j.atmosres.2020.104878.

Søndergaard, J., Bach, L., Asmund, G., 2013. Modelling atmospheric bulk deposition of Pb, Zn and Cd near a former Pb-Zn mine in West Greenland using transplanted Flavocetraria nivalis lichens. Chemosphere 90, 2549–2556. https://doi.org/10.1016/j.chemosphere.2012.10.097.

Vázquez-Arias, A., Martín-Peinado, F.J., Parviainen, A., 2023. Effect of parent material and atmospheric deposition on the potential pollution of urban soils close to mining areas. J. Geochem. Explor. 244 https://doi.org/10.1016/j.gexplo.2022.107131.

Widory, D., Vautour, G., Poirier, A., 2018. Atmospheric dispersion of trace metals between two smelters: an approach coupling lead, strontium and osmium isotopes from bioindicators. Ecol. Indicat. 84, 497–506. https://doi.org/10.1016/j.ecolind.2017.09.003.

Zuluaga, M.C., Norini, G., Ayuso, R., Nieto, J.M., Lima, A., Albanese, S., De Vivo, B., 2017. Geochemical mapping, environmental assessment and Pb isotopic signatures of geogenic and anthropogenic sources in three localities in SW Spain with different land use and geology. J. Geochem. Explor. https://doi.org/10.1016/j.gexplo.2017.07.011.